RSC Advances



REVIEW

View Article Online
View Journal | View Issue



Cite this: *RSC Adv.*, 2022, **12**, 11750

# Fabrication and prospective applications of graphene oxide-modified nanocomposites for wastewater remediation

Faiza Asghar, *[a] Bushra Shakoor,[a] Saira Fatima,[b] Shamsa Munir, [c] Humaira Razzaq,[a] Shazia Naheed[a] and Ian S. Butler[d]

Water bodies have become polluted with heavy metals and hazardous contaminants as a result of fast development. Many strategies have been devised by researchers in order to remove hazardous contaminants from the aquatic environment. Utilizing graphene oxide-based composite materials as efficient adsorbents for waste water treatment, desalination, separation, and purification is gaining attraction nowadays. Some of their defining properties are high mechanical strength, hydrophilicity, remarkable flexibility, ease of synthesis, atomic thickness, and compatibility with other materials. In water treatment, high separation performance and stable graphene-based laminar structures have been the main goals. Magnetic separation is among the methods which received a lot of attention from researchers since it has been shown to be quite effective at removing harmful pollutants from aqueous solution. Graphene oxide-modified nanocomposites have provided optimal performance in water purification. This review article focusses on the fabrication of GO, rGO and MGO nanocomposites as well as the primary characterization tools needed to assess the physiochemical and structural properties of graphene-based nanocomposites. It also discusses the approaches for exploiting graphene oxide (GO), reduced graphene (rGO), and magnetic graphene oxide (MGO) to eliminate contaminants for long-term purification of water. The potential research hurdles for using fabricated MGOs as an adsorbent to remediate water contaminants like hazardous metals, radioactive metal ions, pigments, dyes, and agricultural pollutants are also highlighted.

Received 14th January 2022
Accepted 4th April 2022

DOI: 10.1039/d2ra00271j

rsc.li/rsc-advances



[a]*Department of Chemistry, University of Wah, Quaid Avenue, Wah 47040, Pakistan. E-mail: dr.faiza.asghar@uow.edu.pk*
[b]*Department of Chemistry, Quaid-i-Azam University, Islamabad, Pakistan*
[c]*School of Applied Sciences and Humanities, National University of Technology, (NUTECH), Islamabad, 44000, Pakistan*
[d]*Department of Chemistry, McGill University, Montreal, QC H3A 2K6, Canada*

*Dr Faiza Asghar is working as an Assistant Professor in University of Wah, Pakistan. Her research work focusses on the areas of unmet clinical needs i.e. cancer, diabetes, and antimicrobial infections and she is also working on wastewater remediation. As a dedicated researcher having an excellent academic profile she obtained her PhD degree availing fully funded scholarship from the Higher Education Commission (HEC) of Pakistan, and partial PhD research work at the prestigious McGill University, Canada. She published her research work in well reputed and good impact factor international journals such as RSC, Elsevier, Frontiers, and Wiley. Dr Faiza's research work is augmented with the new strategies in the areas of synthesis, medicinal chemistry, spectroscopy, electrochemistry, and structural chemistry. Her expertise in a wide range of spectroscopic techniques such as FT-IR, NMR, GC-MS, and in analyzing and processing the data using different softwares is commendable.*

*Ms. Bushra Shakoor obtained her MS degree in Inorganic Chemistry at the University of Wah, Pakistan. She is currently a PhD student under the supervision of Dr Faiza Asghar at University of Wah, Pakistan. Her research focuses on the development of medicinally active compounds and its applications in medical field.*

# 1. Introduction

Fresh water is required for all forms of life, but fresh water is only 3% of earth's overall resources as compared to sea water *i.e.* 97%. Out of this only 1.2% is drinkable; the rest is locked up in glaciers, ice caps *etc.*[1] Only a small fraction of earth's fresh water is found in liquid form.[2] A large fraction of the earth's water is salt water.[3]

The available freshwater is decreasing due to rapid global population, climate change, urbanization, industrialization and more stringent health-based water qualities.[4] By 2050, the population is expected to increase from 7 to 10 billion, and as a result industrialization, and water pollution will also elevate. According to the report by United Nations World Water Development, around 748 million people do not have access to pure drinking water. According to the statement by the World Health Organization (WHO) in 2002, deficiency of clean and secure water accounted for 3.1% of deaths across the world.[5] Our planet faces enormous hurdles in addressing the growing demand for clean water. Across the globe, the increasing scarcity of freshwater has urged the need for the development of revolutionary water supplies that includes desalination of sea water, reutilization and reprocessing of wastewater and water from storms.[6,7] Sea water is the most abundant supply of drinking and industrial water on the planet, but it cannot be used for domestic purposes due to its high salinity. To make it drinkable salts need to be removed by a process known as desalination, making it applicable for drinking purposes.[8]

One of the main causes of water pollution is organic pollutants from the industrial, agriculture, and domestic waste that contaminates water. These contaminants present in water are very harmful for human beings and also for the aquatic life, because the accumulation of these contaminants develops high risks for human health as all these enter the human body through water consumption and cause diseases in humans that include human hepatic dysfunction, carcinogens hindering the development of the human body and endangering the human endocrine system. Water pollution is the problem of the entire world.[9]

## 1.1 Membrane-based separation technology

In the past decades, membrane-based separation technology has gained value in water purification due to its positive impact on the environment, energy efficiency and easy use. We can categorize the membrane-based desalination process on the basis of pore size of the membrane and rejection mechanism as: Membrane Distillation (MD), Electro-Dialysis (ED), Ultra-Filtration (UF), Micro-Filtration (MF), Nano-Filtration (NF), and Reverse Osmosis (RO).[10]

One of the membrane-based desalination techniques is reverse osmosis (RO) which is considered as one of the best technologies to purify sea water. It is usually used instead of thermal desalination methods[11] including multistep flash and multiple effect desalination, because these techniques are not energy efficient. The energy consumption of RO has decreased from 5 kW h $m^{-2}$ in the 1990s to 1.8 kW h $m^{-2}$ today, compared to other methods.[12] Therefore, RO desalination is expected as a sustainable solution to address the worldwide water supply crisis.[13]

## 1.2 Challenges for water desalination membranes

Water desalination using membranes suffers from a number of challenges. Membrane fouling is a major challenge in desalination technology, and RO membrane performance has

*Dr Saira Fatima has completed her PhD & MPhil degree from Quiad-i-Azam University Islamabad in Inorganic/Analytical Chemistry in 2020. My dissertation title was "Study of new ferrocene based Thioureas as potential amphiphiles and corrosion inhibitors". Dr Saira research interests lie in the field of synthesis of multifunctional organometallic compounds and their metal based self-assemblies, electrochemistry and their computational studies. She has made eleven scholarly contributions including fourteen peer-reviewed research articles in reputed international SCI journals.*

*Dr Shamsa Munir, Assistant Professor in Chemistry at School of Applied Sciences and Humanities, National University of Technology, Islamabad, Pakistan, earned PhD from Quaid-i-Azam University, Islamabad. Her research expertise includes hybrid bulk heterojunction solar cells, electrochemical fuel cells, and synthesis of nanomaterials for various applications such as electrode materials and photocatalysis. She has published research papers in reputed international journals. Sustainable energy technologies are the focus of the present-day researchers due to the scarcity of the fossil fuels as energy providers. Solar energy is the only way out to overcome this energy crisis providing solution in numerous forms such as solar cells, photoelectrochemical degradation of waste materials and photoelectrochemical production of fuels. Her current ambitions are to contribute to this evolving field of renewable energy by fabricating efficient and cost effective materials.*

*Dr Humaira Razzaq is Assistant Professor in University of Wah since 2018. She started her professional carrier from National centre of physics as an Assistant professor and worked as a research fellow. She is a competitive researcher and have many research collaborations. Her major research interests include synthesis of nanomaterials and their electrochemical properties, development of polymer Nano-composites and polymeric membranes for waste water remediation. Recently, she won the NRPU project of HEC worth of 8.2 million PKR.*

suffered as a result.[14,15] Membrane fouling can be caused by one or both of the mechanisms:

(a) Membrane pore fouling.

(b) Membrane fouling on the surface.

The presence of contaminants in feed water, such as biogenic materials, suspended inorganic or organic debris, and dissolved particles, causes membrane surface fouling.[16] The biological contaminants accumulating on the membrane surface during the RO process and forming biofilms[17] are major limiting issues in the desalination of sea water.[18]

Disinfectants such as chorine are used to eliminate developing biofilms, however they might react with polyamide (PA) on the membrane surface layer.[19–22] Even at low chlorine concentrations, the interaction of chlorine with PA causes changes in the function of thin film composite (TFC) of the RO membrane.[23]

There is a necessity to fabricate effective membranes because the polymeric membranes used in RO suffer from flux drop under high pressure, low tolerance to chlorine, acids and alkalis, and high temperature.[24] Problems with performance restrictions and the post-treatment procedure are still being investigated. Carbon-based materials, nanostructures such as zeolites, and ceramics are replacing polymeric membranes, and they are gaining attention due to their high rejection rates, high flux, and chemical resistance.[25–27] But these materials also have certain limitations such as the zeolite membranes failed because these are uneconomical to fabricate on a broader scale due to reproducibility, and fault synthesis.[17,20] While ceramic membranes have also limited practical applications in membrane technology as they are very expensive and brittle under high pressure.

Carbon nanotubes (CNTs) are also less attractive due to high cost and impure synthesis and operational issues have prevented its study and making it difficult to develop CNTs into large area membranes.[28,29] Synthesizing high purity CNTs is a major challenge in today's world. Purification is a critical issue to address since as-prepared CNTs are generally accompanied by carbonaceous or metallic contaminants. Carbonaceous impurities and metal catalyst particles in CNTs generated by arc discharge, laser ablation, and chemical vapor deposition (CVD) are unavoidable, and the number of impurities often increases as the diameter of the CNT decreases. The main disadvantages of the arc discharge method are low purity, a high destroying rate of starting materials (95%) and high reactivity of the remaining nanotubes at the end of the process due to the presence of dangling bonds (an unsatisfied valence), which requires high-temperature annealing (2800 ± C) to eliminate. Because the carbon source in arc discharge and laser ablation comes from vaporization of graphite rods, some un-vaporized graphitic particles that fall off the graphite rods frequently appear as impurities in the final product.[30]

The most difficult problem is removing polyhedral carbons and graphitic particles that oxidize at the same rate as CNTs, particularly SWCNTs. Transition metal catalyst residues are the most common source of metal contaminants. Carbon layers (ranging from disordered carbon layers to graphitic shells) encase these metal particles, rendering them impervious to acids and preventing them from dissolving. Another issue to address is that carbonaceous and metal impurities have a wide particle size distribution and varying quantities of flaws or curvature depending on synthesis circumstances, making it challenging to establish a unified purification process for consistently high-purity CNT materials. Purification of the as-prepared CNTs is critical in order to meet the huge potential applications and to research the fundamental physical and chemical properties of CNTs.[31]

For industrial and research applications of graphene and reduced graphene oxide (rGO), large-scale manufacturing is important.[32] Chemical solution approaches provide a low-cost, high yield alternative for producing rGO compared to CNTs (Table 1).

During the last few years, chemically modified graphene (CMG) has attracted great interest in the perspective of several applications such as sensors, energy related materials, polymer composites, field effect transistors (FET), paper-like materials, and biomedical relevance due to remarkable mechanical, thermal and electrical, properties. Carbon nano-fillers are used in many applications due to their remarkable electrical, thermal and mechanical properties which have been determined both theoretically and experimentally.[32] Advantages and disadvantages of graphene oxide, reduced graphene oxide and carbon nanotubes are presented in Table 2.

Nanomaterials offer a perplexing combination of great performance and limiting constraints. They are an important topic for creating and preparing high-efficiency, reusable green adsorbents to increase the adsorption and removal of water contaminants using graphene oxide-based materials. This research serves as a guide for removing heavy metals from wastewater in order to reduce water pollution and facilitate ecological building.[42]

Mechanical, electrical, thermal, and surface properties of graphene, graphene oxide, and reduced graphene oxide (rGO) are all outstanding. Due to its huge surface area (2600 $m^2 g^{-1}$), graphene has been shown to be an excellent choice as an adsorbent for the removal of dyes, metal ions, oils, chemical compounds, and other contaminants. The honeycomb structure of graphene oxide is made up of $sp^2$ hybridized carbon with oxygen containing functional groups like carboxyl, epoxy, keto, and so on. This honeycomb like lattice generally repels water, but when narrow pores are made in it, rapid water diffusion is permitted. As water molecules pass, contaminants are blocked. So, GO sheets are preferred for water treatment purposes.[43]

The adsorption technique using a solid adsorbent offers the low installation cost and easy operation with high efficiency and an environmentally friendly and affordable make it one of the preferred methods for water purification.[44] Thus, graphene oxide played a dominant role as a proficient adsorbent for wastewater treatment in a number of studies. However, good dispersive property of GO in aqueous phases has been regarded as an obstacle for separating and retrieving the adsorbent for reuse after treating heavy metals. To address this flaw, the GO has been cross-linked with polymers to prevent it from leaching into water. The problem of facile separation after water treatment is not solved by simply functionalizing GO with polymer

Table 1 Effective costs involved in producing CNTs, GO and rGO by various methods

| CNT | GO | rGO |
|---|---|---|
| Conventional arc discharge in vacuum: Tungsten Inert Gas (TIG) power source, inert atmosphere, metal cabinet with water cooling system, automated process and chemical purification.[35] Cost: 15$ per g | A top-down process involved the chemical oxidation of the precursor graphite powder (size ~10 μm) using a concentrated mixture of sulphuric acid and nitric acid. Oxidized graphite powder was thermally exfoliated at 1050 °C for 30 s to produce graphene oxide (GO). Cost: It can be produced using inexpensive graphite as raw material by cost-effective chemical methods with a high yield[33] | Microwave and photo reduction: by treating graphite oxide powders in a commercial microwave oven, rGO can be readily obtained within 1 min in ambient conditions.[33] Cost: low-cost, high-yield protocol |
| Chemical vapor deposition (CVD): furnace, inert atmosphere, metal catalyst.[35] Cost: 40$ per g | | Chemical reduction: chemical reduction in GO sheets with sodium borohydride led to the formation of rGO.[34] Cost: Low-cost, high-yield protocol |
| Laser ablation: laser source, furnace, inert atmosphere, metal catalyst-graphite composite.[35] Cost: due to high capital cost of the laser and the fewer quantity of CNT after final purification, this method is not commercially viable | | |
| Floating catalyst method: tubular reactor, quartz tube, thermocouples, inert gas.[36] Cost: it needs a complicated set up. The cost of aromatic hydro carbons is very high (benzene: 44$/10 g) | | |
| Electrical Discharge Machining (EDM) process: plasma sputtering unit, Microelectric discharge apparatus, metal catalyst.[36] Cost: it requires costly equipment such as plasma sputtering unit and micro electric discharge unit | | |
| Simplified arc discharge in air: manual metal arc welding machine and chemical purification.[36] Cost: 3$ per g | | |

molecule. The GO layers can be immersed in the crosslinked alginate matrix to alleviate the issue of adsorbent leaching, according to reports. The GO layers are physically trapped in the beads during this procedure. GO, on the other hand, has no chemical bonds with the polymer matrix or any other characteristics that might improve the stability and adsorption capacity of a GO-based adsorbent. The GO layers are crosslinked and the availability of ligating groups for metal ion complexation can be exploited by employing multifunctional polyamine for the modification. As a result, sodium alginate was employed as a polymer matrix for the GO dispersion, and GO was then functionalized and reduced concurrently using polyethylenimine (PEI). The bonds in GO become locked or totally bound after functionalization with PEI, boosting GO's reusability, efficiency, and stability.[45]

The magnetization of GO is another best solution to avoid the above problem, whereby using the external magnetic field, magnetized GO can be easily separated. In addition, magnetic materials not only have the advantage to easy and rapid separate from aqueous solution but also shows high adsorption capability towards pollutant. This is a most significant factor for an efficacious separation to identify a suitable magnetic adsorbent material that will dominate the selectivity of the technique.[46]

Graphene and GO-based membranes are thought to be next-generation separation materials for applications in water purification due to their significant intrinsic mechanical strength, excellent antibacterial activity, and perfect antifouling capabilities.[47,48] The research is focused on graphene-based materials, and improvement in the molecular simulation of graphene lineage have paved the way for new membrane desalination techniques to be developed.

### 1.3 Graphene

Graphene is a rapidly growing star on the horizon of materials science and condensed-matter physics. Despite its brief history, this purely two-dimensional material has remarkable crystal and electrical quality, and has previously disclosed a plethora of advance physics and prospective approaches.[49] It possesses broad surface area, high absorption capacity, high electrical conductivity even 13 times better than that of copper (~5000 W $m^{-1}$ $K^{-1}$), and thermal conductivity twice times better than diamond.[50]

Graphene is typically classified as a few layer structure such as single-walled, double-walled and multi-walled carbon nanotubes shown in Fig. 1. This is due to its most essential feature that is incredibly adaptable carbon backbone, which enables for simple functionalization and integration in a wide range of application.[51] It can also be easily fabricated to be used on a large scale, as evidenced by recent work on the production of 30 inch multilayer sheets of graphene and

Table 2 Comparison between graphene oxide, reduced graphene oxide and carbon nanotubes

| | Graphene oxide/reduced graphene oxide/carbon nanotubes | |
|---|---|---|
| S. no. | GO/rGO | CNTs |
| 1 | Graphene oxide contains reactive oxygen with functional groups like carboxylic, hydroxyl, and epoxy. These functional groups not only make the layers hydrophilic, but they also increase the interlayer distance; single layer GO sheets are reported to be 1–1.4 nm thick[37] | Many studies have been conducted to adjust the surface features of CNTs using various approaches; nevertheless, many procedures and material variables have yet to be thoroughly optimized[38] |
| 2 | Because of the presence of these functional groups, GO is highly hydrophilic in nature, dispersing up to 3 nm $mL^{-1}$ in water with ease and allowing water molecules to easily intercalate between GO sheets[37] | Because of the projected negative impacts, concerns about structural changes arising from chemically functionalizing CNTs, the harmful effects of ultra-sonication, and other dispersion and mixing processes remain[39] |
| 3 | As graphene oxide is already functionalized so its aspect ratio does not get disturbed[38] | CNT has a higher aspect ratio than 1000, however following functionalization, the aspect ratio got disturbed[39] |
| 4 | Individual GO sheets that result are mainly single or few layer sheets that disperse easily in water to form a stable colloidal GO solution. The aqueous GO colloidal suspension provides an ideal environment for converting GO to electrochemically reduced graphene oxide *via* an electrochemically technique (ERGO)[39] | Methods for modifying their surface properties are being developed. Chemical functionalization and physical approaches based on interactions between active molecules and carbon atoms in nanotubes can be appropriately split[43] |
| 5 | Negative electrostatic repulsion caused by ionization of phenolic hydroxyl groups and carboxylic groups is thought to be responsible for the GO suspensions stability[40] | Researchers discovered that when tubes in a liquid suspension disperse, they stick together. Chemical processes cause CNT to re-agglomerate in the matrix<br>They are ineffective in transferring load across the matrix–nanotube interface[41] |

transport on roll-to-roll fabrication.[52] Dr Konstantin Novoselov[53] and Prof. Andre Geim[54] were the first to mechanically exfoliate graphene from graphite using a simple scotch tape method in 2004. Graphene is the basic building element of graphite, which is made up of sheets of graphene layered together with an interlayer spacing of 3.34 angstrom.[55] By coming into direct contact with microorganisms, graphene and carbon nanotubes can impede their growth. CNTs are a younger generation of nanomaterials when compared to the nanomaterials covered previously. CNTs were discovered and described for the first time in 1952, and then again in 1976.[56] Iijima is credited with being the first scientist to report the formation of multi-walled carbon nanotubes (MWCNTs) following a random even during arc evaporation of C60 and other fullerenes in 1991. Carbon nanotubes (CNTs) are carbon tubes that possess diameter measured in nanometers. Single-wall carbon nanotubes (SWCNTs) with dimensions in the nanometer range are generally known as carbon nanotubes. Carbon nanotubes with a single wall are an allotrope of carbon that lies halfway between fullerene cages and flat graphene.[57]

Graphene oxide (GO), reduced graphene oxide (rGO), graphite (Gt), graphite oxide (GtO), and magnetic graphene oxide (MGO) are shown in Fig. 2. When contrast the antibacterial activity different graphene-based materials against *Escherichia coli* (bacterial species), at the same concentration, length of incubation, and environmental conditions. GO

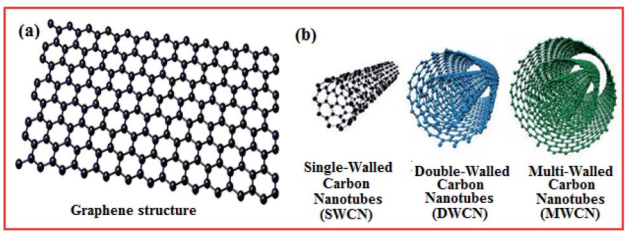


Fig. 1 (a) Structure of graphene (b) structure of single, double and multi-walled carbon nanotubes.

dispersion outperforms the others. Instead of using graphene alone, it is better to use graphene oxide, which has better oxidative properties than graphene, or nanoporous graphene (NPG).[58,59] Graphene-based materials are employed in a variety of applications, but we will concentrate on water purification.[60]

### 1.4 Nonporous graphene membrane (NPG)

NPG membranes are also strong candidates in wastewater remediation. Various experimental approaches have been presented, and substantial advancements have been made, in order to introduce nano holes into graphene. Ion bombardment and oxidative etching procedures can be used to define sub-nanometer sized pores in graphene with high precision.[61,62] It

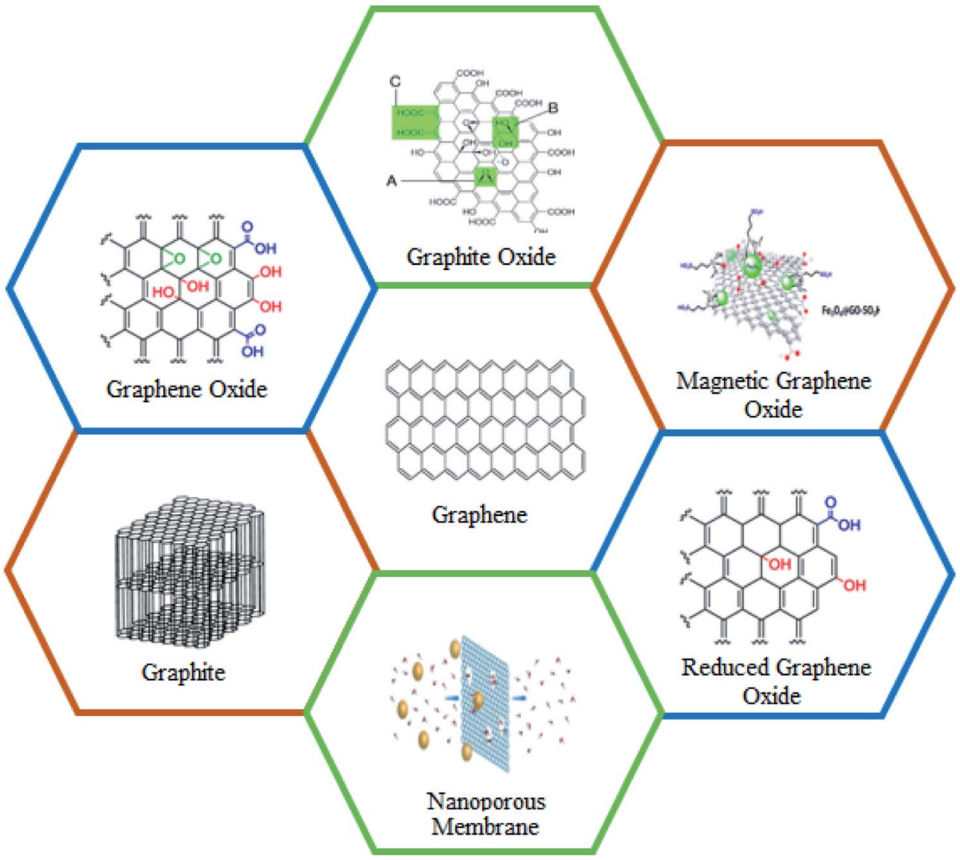


Fig. 2 Graphene-based materials.

has the potential to reject 100% of salt.[63] The porosity of graphene can be adjusted to control water permeation rates.

As a result of the nano pore morphology, NPG has the ability to produce high water flow rates shown in Fig. 3 as well as salt rejection, but single layer graphene sheets are difficult to assemble. So, achieving large NPG membranes can be manufactured in a scalable manner and cost effectives with a required pore size, keeping graphene's intrinsic structural integrity while narrowing the size distribution remains a serious problem.[64] The disadvantages of NPG for desalination include the difficulty of achieving a narrow size distribution of holes with high density, as well as the fact that these tiny shafts produced in graphene limited the permeation of water. The entire process of composing NPG requires extreme caution, even if a high degree of water permeability is attained. High density shafts can reduce mechanical qualities or perhaps destroy the entire structure. Finally, oxidative etching, high quality graphene design, and ion bombardment are all expensive processes.[65]

## 2. Synthesis of graphene-based materials

### 2.1 Graphene oxide (GO)

Membrane technology is a fast developing field with a variety of real-world applications, including desalination and purification of water. Scientists and engineers are developing this technology in order to create a membrane that is more cost effective and efficient. Dikin *et al.*[66] were the first to develop GO as a viable membrane, discovering that stacking graphene oxide films allowed for a unique water penetration channel while selectively hindering the movement of gases and non-aqueous solutions. Graphene-based materials, particularly graphene oxide, have been extensively researched for thin film and membrane applications due to their 2D structure, one atom thickness, and good mechanical strength and flexibility.[67,68] Because GO has a large surface-to-thickness ratio, it has become an important material to design ultra-thin and high-perm selective membranes.[69,70] GO fragments can simply be stacked on top of one another to form a membrane. It allows water to flow through it but not vapors to travel through.[71] Nothing can travel through graphene, although it has super membrane qualities and is economically employed. The progress of graphene oxide (GO) and reduced graphene oxide (rGO) has made them suitable for water treatment.[72–75]

**2.1.1 Preparation of GO.** Graphite oxides (GtO) are common precursors for producing graphene oxide dispersions in water and other solvents.[62] After that, graphene oxide dispersions can subsequently be deposited into multilayered graphene oxide structures, shown in Fig. 4 chemically altered with solution-based techniques, or reduced to make a variety of graphene related materials for multifunctional applications. GO membranes are used to purify water and can be

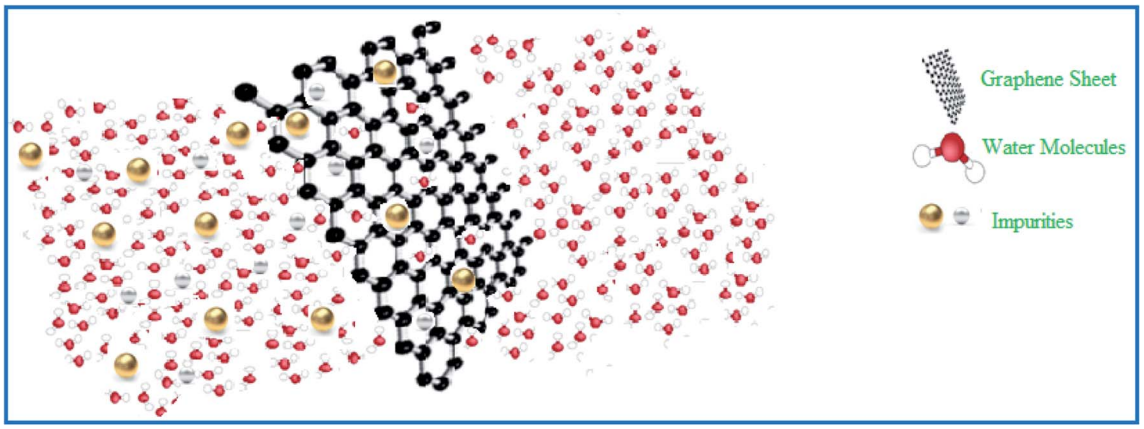


Fig. 3 Nano porous graphene membrane.

manufactured in a variety of ways, including Brodie,[76] Staudenmaier,[77] and the Hummers' method.[78] The first two processes use nitric acid ($HNO_3$) and potassium chlorate to oxidize graphite ($KClO_3$). For manufacturing graphite oxide, the Hummer process provides a faster, safer, and more competent method. The use of concentrated nitric and sulfuric acid in the manufacture of GO was hazardous before this technology. Heo *et al.* used a modified Hummer technique to fabricate GO. This method uses a mixture of $KMnO_4$ and $H_2SO_4$ to oxidize graphite.[78,79] Intercalating graphite with acids produces the salts such as sulphuric acid ($H_2SO_4$) and nitric acid ($HNO_3$), which are made before the exfoliation stage.

Graphene oxide can be fabricated mainly in two steps:

(a) Through graphite oxidation.

(b) *Via* graphite oxide exfoliation.

Graphite powder (Gt) is oxidized to generate graphite oxide (GtO), which due to the presence of hydroxyl and epoxide groups across the basal planes and carbonyl and carboxyl groups at the edges, is easily distributed in water or another polar solvent.[80,81] Second, sonication can be used to exfoliate bulk graphite oxide, yielding colloidal suspensions of monolayer, bilayer or few layer graphite oxide sheets in a variety of solvents.[82] Exfoliation is the process of converting stacked graphite layers into single graphene layers.[83] The choice of appropriate oxidizing agents to oxidize graphite is a vital part of the GO preparation process. Due to the presence of –OH, –COOH, –C–O–C–moieties, graphene oxide (GO) can stretch further. The hydrophilicity of GO is unbreakable. It offers a broader range of applications than graphene.

**2.1.2 Applicability of GO-based membranes.** Membranes made of GO can be utilized in the following ways:

*2.1.2.1 Self-supporting (GO directly used for separation).* Xu *et al.*[84] described a continuous vacuum filtering approach for fabricating free-standing GO membranes with gaps between GO nano sheets. The pore size of the GO/$TiO_2$ composite nano filtration (NF) membrane was 3.5 nm on average. They used $TiO_2$ nanoparticles to expand the distance between the nano sheets and create channels. This NF GO/$TiO_2$ membranes has a desertion rate of nearly 100% for pollutants in water. GO/$TiO_2$ sheets were layered into well-packed GO/$TiO_2$ membrane arrangements. These $TiO_2$ nanoparticles might reinforce GO nanosheets, thereby increasing the interlayer spacing, resulting in the creation of pores and appropriate channels in the manufactured membranes, making them promising water filtering

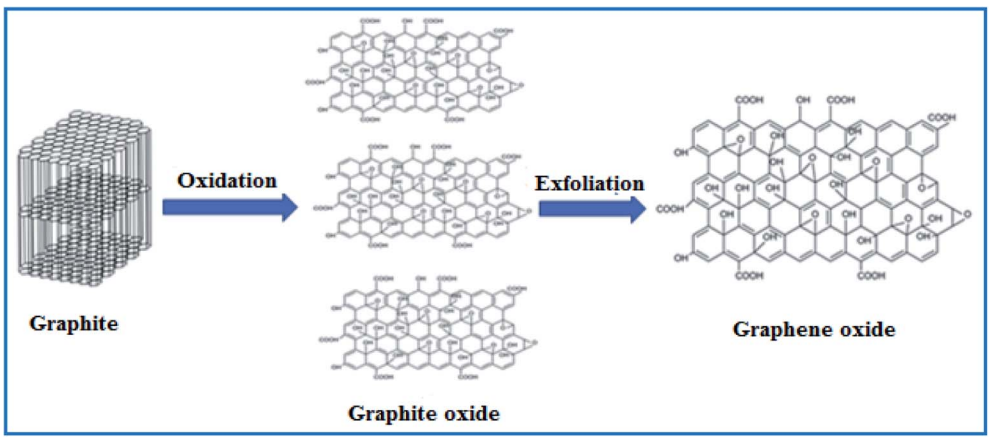


Fig. 4 Synthesis of graphene oxide.

membranes.[85] Nair *et al.* reduced the inter-sheet gap to about 1 nm, and his research included fabricating free-standing Cu-accommodated GO nano filtration membranes using spray or spin coating method, with the resulting membranes being completely impermeable to gases, vapors, and liquids, as well as helium gas, while enabling water to flow. Furthermore, water permeates at a rate 1010 times faster than helium.[86] Sun and colleagues produced GO freestanding NF membranes with inter-sheet spacing of 0.82 nm using drop casting procedures, and these membranes can easily filter sodium salt from copper salt and organic impurities. Because of their ultrathin thickness (10 nm), freestanding GO membranes have a remarkable ability to flotsam salt by 100% while simultaneously having significant water permeability and penetration ability nearly double that of conventional RO approaches.[87]

*2.1.2.2 Supported by polymeric or inorganic substrate.* The properties of the GO could be improved if it is correctly integrated with ceramic, polymer matrices, or substrate. Membranes with GO are utilised in a variety of applications, including:

(a) Fuel cells,[88,89] nano filtration,[90,91] ultra filtration,[92,93] pervaporation[94,95] are some of the topics that have been discussed.

(b) The antifouling, mechanical, and surface charge properties of the resultant hybrid polymer membrane can all be improved by GO. The hydrophilic characteristic of specific moieties in GO improves GO membranes and enables improved GO distribution in water and organic solvents, resulting in a mesh-like structure of GO layers at nanoscale.

(c) Water molecules are absorbed at –OH first, then diffuse across the hydrophobic carbon core, forming water channels that enhance penetration flux. When water molecules invade GO layers, they form one-layer organization that pushes the other layer apart, increasing the *d*-spacing.

*2.1.2.3 Substrate effect.* The substrates bulk pore structure, as well as its surface morphological and chemical structure, affects the interfacial adhesion and nano filtration performance of the GO membrane. Due to number of oxidized moieties in polyacrylonitrile (PAN),[96] interfacial adhesion of the GO membrane is improved, and the extremely porous sublayer with flat skin allows for very low transport resistance, resulting in outstanding nano filtration performance of the GO membrane. The PAN substrate has a pore size of 20 nm, a very thin, dense top layer that is about 1 μm thick, and a finger-like cylindrical pore structure with enormous tubular macro spaces at the bottom.

These features provide a level platform for GO laminate assembly as well as wide water penetration channels. This PAN substrate had a water penetration of 585 L $m^{-2}$ $bar^{-1}$, which was more than 5 times that of the ceramic substrate. The polycarbonate (PC)[97] substrate has a very high water permeability due to its circular straight through holes, yet it has a very poor adhesion performance due to the lack of surface functions. Because of its low transport resistance, a PC substrate with pore size of 200 nm and ultrahigh water permeances of 4575 L $m^{-2}$ $bar^{-1}$ exhibits straight pore channels with little tortuosity through its bulk structure, while interior pore channels of PC collapse readily and induce deformation and even a fracture in the bulk pore structure.

*2.1.2.4 Modified composite membrane.* In order to increase water permeability, mechanical strength, and antibacterial characteristics, recent research has been conducted. GO must be combined with polymers before being cast. Polymer solutions such as polyvinylidene fluoride (PVDF) and polysulfone (PSF) were combined with functionalized GO (f-GO) and cast together utilizing the phase inversion process.

*2.1.2.5 Water purification using a GO-intensified polyamide (PA) thin film nanocomposite (TFN) membrane.* In the membrane separation field, ultra-thin graphene membranes are utilised to separate gases present in water, hence graphene nanosheets or graphene nanocomposite are used due to their potential application in water purification. For improved separation, graphene is boosted by connecting its derivatives, like graphene oxide and reduced graphene oxide to a polymeric substrate; the resulting membrane outperforms graphene. Ultrathin graphene nano filtration (NF) membrane on top of which microfiltration membrane is put, created by vacuum filtration of reduced graphene oxide. This process can also be used to make a $TiO_2$–graphene oxide membrane.

Another method involves incorporating GO nanosheets into the matrix of polymer. Even though, graphene is incompatible with organic polymers, hydroxyl, epoxide, diol, and ketone-containing GO sheets can alter the interaction between GO sheets and the polymer matrix. The hummingbird approach may be used to make GO nanosheets, which are then interfacial polymerized into a polyamide thin film layer. To build the TFN membrane, GO nanosheets with a multilayer structure were produced and employed as the filters, resulting in nanosheets that were well disseminated in the PA thin film. The hydrophilicity of the TFN membrane increases as the concentration of nanosheets increases, resulting in an increase in water flux. Mixing functionalized hydrophilic nanoparticles with the polymeric matrix can enhance the amorphous nature of the membrane. The penetrability of GO was increased due to the fast exchange of solvent and non-solvent during the phase inversion method. The addition of f-GO improves pore size and porosity, although it decreases as more additives are added.

*2.1.2.6 Filtration mechanism.* GO membranes with a sub micrometer thickness can fully block the flow of liquid and gas molecules, allowing only water vapors to pass through.[98] This could be owing to the presence of empty spaces between non-oxidizing graphene oxide sheets, which allow water vapors to pass through low-friction channels. The following are some of the probable filtration mechanisms for GO membranes:

(a) Size exclusion.

(b) Donnan exclusion.

(c) Adsorption phenomenon.

Massive organic molecules can be strained out due to the existence of nano channels in the membrane. The size of the nano channels must be enhanced for precise separation of bulky molecules and ionic species by changing the spacing between graphene oxide sheets[57] as seen in Fig. 6. We can create graphene oxide membranes with precise spacing in layers for

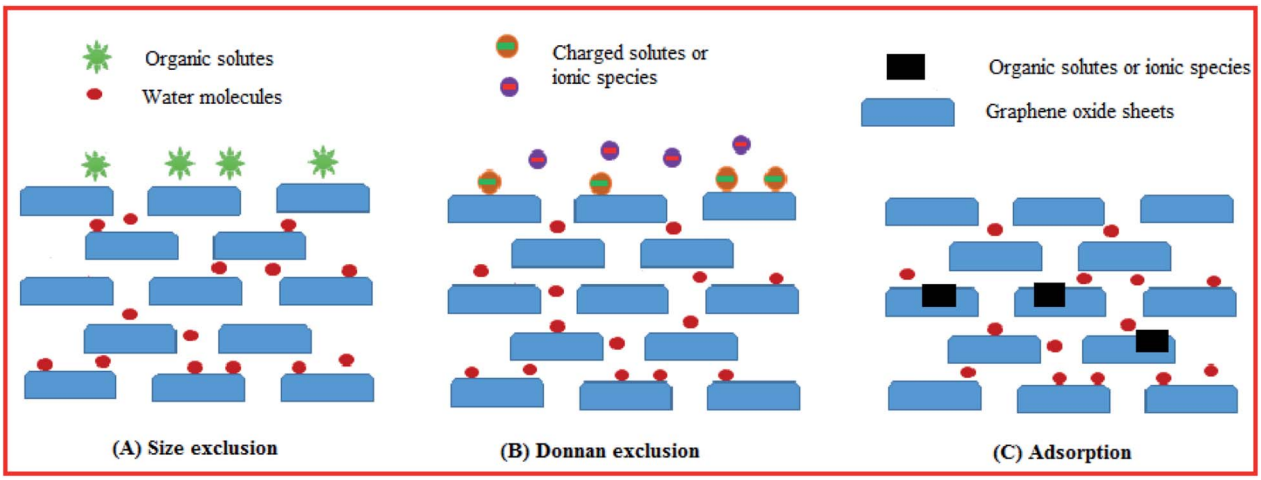


Fig. 5 Filtration mechanism.

required applications such as desalination, water purification, and pharmaceuticals.

The Donnan exclusion process[99,100] can also be used to remove ionic or charged species as shown in Fig. 5. Negatively charged organic species or divalent ions can be rejected by pure graphene oxide membrane in this procedure because GO membrane becomes negatively charged as the proton from the carbonyl group on the graphene oxide sheet's edge or tape is removed.[101]

The adsorption phenomenon is another mechanism. Small ionic species can be rejected by the GO membrane by strong adsorption,[102] as seen in Fig. 5 which involves interactions with different areas of graphene oxide sheets. It is because of the fact that O-containing moieties of graphene oxide membranes[103] form co-ordinates with transition metal cations, resulting in complete blockage, and alkali and alkaline earth metals permeability are also reduced as a result of their relation with $sp^2$ plaster of graphene oxide sheets *via* $\pi$ linkage.[104]

*2.1.2.7 Direct contact membrane distillation.* Membrane distillation (MD)[105] is a low temperature thermal evaporation technique (based on membrane) that produces energy efficient water at low temperatures of 50 to 90 °C. Between the heated feed and the cold permeate in MD, a hydrophobic porous membrane functions as a barrier. It permitted vapors to travel through small holes and on the permeate side, compress, but it did not allow liquid phase to pass through. The membrane is the key to flow and selectivity in this case as shown in Fig. 6. We can improve MD performance by improving membrane architecture.

In the field of medicine, graphene oxide is gaining popularity. However, because a single sheet is hard to manufacture, graphene oxide real-world applications remain a hurdle. We are talking about desalination using direct contact membrane distillation with graphene oxide paralyzed on polytetrafluoroethylene (PTFE), which improves the membrane's result rejection ability and allows for a greater flow of 97 kg $m^{-2}$ or at 80 °C. This increase in flux can be attributed to a number of things.

(a) Selective adsorption.
(b) Nano capillary effect.
(c) Reduce temperature polarization.
(d) Polar functional groups in graphene oxide.

Graphene sheets operate as the adsorption site for water vapors generated by hydrogen bonding. Saltwater clusters are rejected by polyvinylidene fluoride (PVDF). The flux can be increased by preferentially hydroxylating or carboxylating[106] the carbon atom close by to the pore, so the main goal of this study is to immobilize graphene oxide on PTFE membrane to synthesize a high-performance desalination membrane for MD. The overall water permeation rates are increased due to the existence of polar moieties such as epoxy and others. All studies employed sodium chloride, PVDF powder, cyclohexanone, and deionized (DI) water.[107] The membranes employed were graphene oxide single atom layer membranes with a thickness of 35 μm and a purity of 70%, as well as graphene oxide single atom layer membranes with a thickness of 0.2 μm and a non-woven polypropylene support.

## 2.2 Reduced graphene oxide (rGO)

To prepare reduced graphene oxide, we need to reduce the graphene oxide membrane due to existence of hydrophilic moieties on the borders of the graphene oxide surface can cause *d*-spacing to decrease, and reduction removes these functional groups. The reduced graphene oxide is made in one of two ways:

(a) Chemical reduction.
(b) Annealing at a high temperature.

The most effective approach for thermal annealing[108] is the thermal deoxygenation of graphene oxide as shown in Fig. 7, which is aided by a rise in temperature, to eliminate O-based moieties like –OH.[109,110] However, this process consumes a lot of energy and the degree of oxidation is hard to manage. Chemical reduction necessitates a shallow temperature range and the use of reducing agents like metal hydrides, hydrazine, and hydroiodic acid. It is challenging to target these functional groups. Reduced graphene oxide membranes-based nano

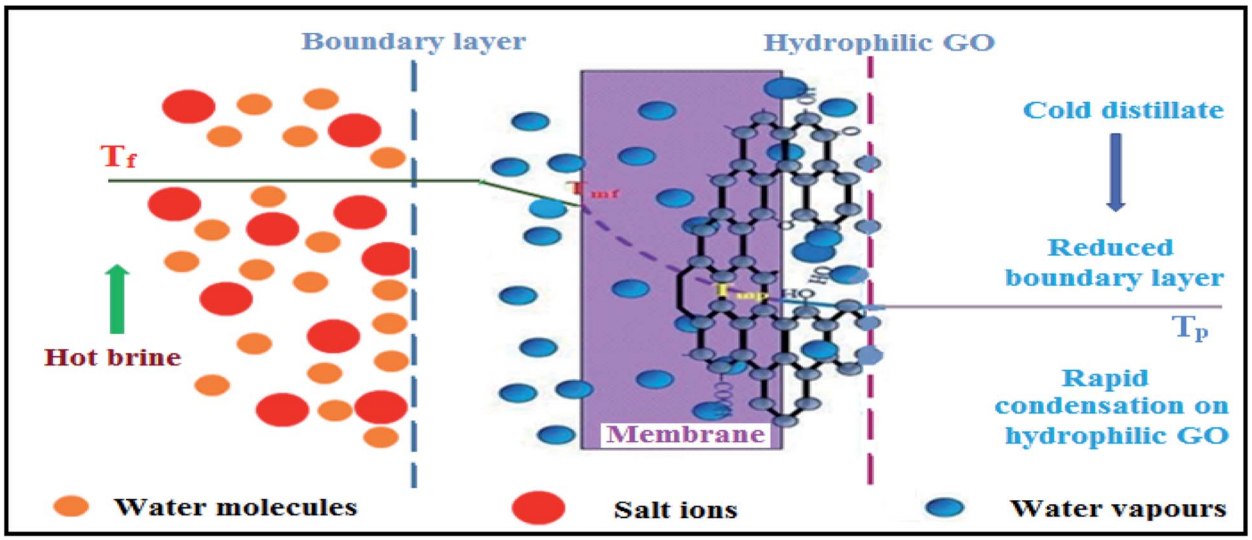


Fig. 6 Desalination across a graphene oxide membrane *via* direct contact membrane distillation.

filtration membranes exhibit superior qualities than graphene oxide, prompting a slew of studies.

### 2.3 Magnetic graphene oxide (MGO)

Due to high dispersibility of graphene oxide it is difficult to isolate it from an aqueous solution, even after the removal of contaminants. The magnetization of GO can solve this problem. An external magnetic field can readily separate the magnetized GO.[111] Furthermore, because the magnetic particles have a high adsorption capacity for pollutants, they are associated with GO. $Fe_3O_4$/GO, rMGO, $Mn_3O_4$/GO, nickel ferrites, and other hybrid nanocomposites have all been created by integrating metal oxides in GO-based nanocomposites. Nickel ferrites are superior to iron ferrites as reaction medium because they have a more catalytic and charge transfer efficiency through $Ni^{+2}$.

## 3. Applications in sustainable water purification

GO is a good adsorbent because it has lot of hydrophilic attachments and high surface area. Because it has an O-containing moieties, GO is more hydrophilic than graphene and forms a more stable complex with pollutants, making it easier to disperse in solution. However, GO has a problem with recovery, which can be solved by using different approaches already discussed in Sections 1.2 and 2.3.

### 3.1 Pollution from agriculture

**3.1.1 Pesticides.** When pesticides are used excessively to kill insects, they accumulate and their residues pollute soil, crops, and vegetables, which is harmful to human health.[111] Neonicotinoid insecticides, such as dinotefuran, clothianidin,

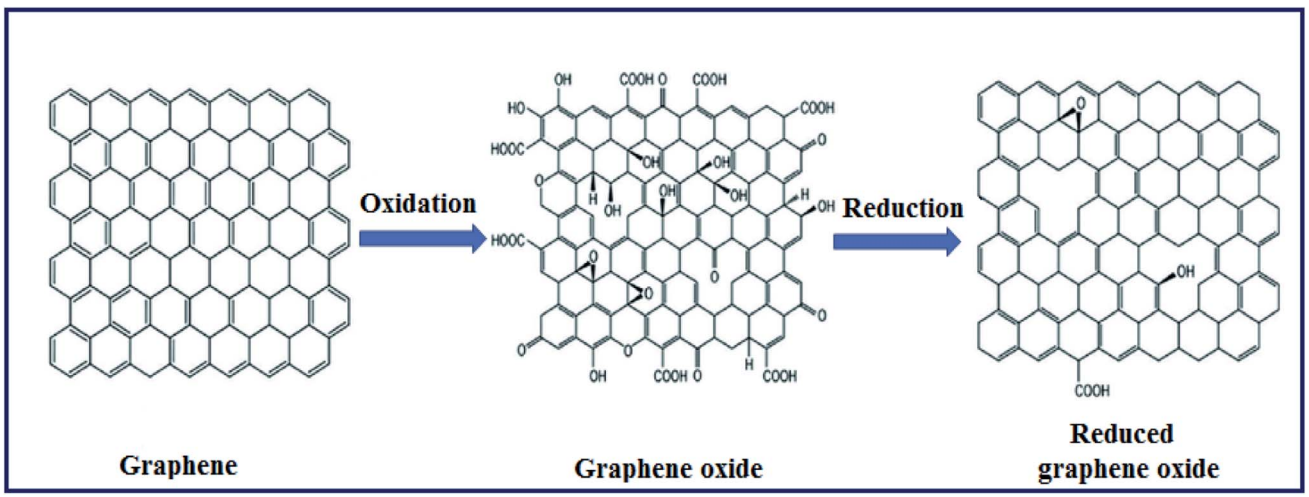


Fig. 7 Synthesis of reduced graphene oxide.

and imidacloprid, are among these pesticides. Liu *et al.*[112] created a magnetic Cu-based metal organic framework (MOF) with $Fe_4O_3$–GO nanocomposite as a support, which they used for adsorption and separation of these pesticides.

**3.1.2 Herbicides.** Atrazine is a weed killer or herbicide that is used in crops like maize, sugarcane, barley to shut out pre and post exposure of weeds, but it is also used in turps such as residential lawns and golf courses to eliminate weeds. However, these chemicals can enter water bodies through rain water and have a negative impact on amphibian sexual development as well as human reproduction. To remove atrazine from aqueous solution by adsorption. Using g-$C_3H_4$–$Fe_3O_4$ as a support, Liu *et al.*[112] created magnetic molecularly imprinted polymer (MMID). Boruah *et al.*[113] developed a $Fe_3O_4$-assisted rGO nanocomposites to eliminate hazardous pesticides such as; simazine, simeton and ametryn.

### 3.2 Organic pollutant removal

Organic pollutant removal can be used to remove dyes, pigments and methadone from the waste water.

**3.2.1 Opioids.** Methadone are commonly used to relieve pain and are available on the market as dolophine, as maintenance therapy, or to treat persons who are addicted to opioids. Due to illegal drugs, this is detected in extremely small concentrations in waste water.[112] Kumar *et al.* investigated the use of MGO as an adsorbent to remove methadone from the environment. Co-precipitation was used to make this MGO-based nanocomposite. Their research found that the $q_{max}$ for methadone elimination was 87.2 mg $g^{-1}$ at the best pH, temperature, and adsorbent dosage, which were 6.2, 295.7 K, and 0.0098 g, respectively.[105]

**3.2.2 Pigments and dyes.** Dyes and pigments are organic compounds that are released by businesses such as paper, textile, paint, and leather, which utilise dyes to colour their products, but the dyes end up in the water. These dyes and pigments are extremely damaging to aquatic life because they hinder sunlight from reaching waterborne plants, reducing photosynthesis, and causing cancer and mutation in humans. Methylthioninium chloride, methyl orange, malachite green, congo red, Persian orange, reactive orange twelve, and other dyes are commonly discovered in waste water.

The following are some of the ways for removing coloured chemicals from effluent or waste water: photocatalytic degradation, electrolysis, adsorption, membrane separation

(a) Adsorption is a highly efficient and simple dye removal process.

(b) Adsorbents based on magnetic nanoparticles are increasingly being utilised to remove hazardous dyes and heavy metals from aquatic environments, however these exposed particles are easily oxidized in the atmosphere. As a result, several methods for functionalizing nanoparticles have been devised to avoid this, and graphene is associated with them due to its unique features.

(c) Because heavy metals and dyes coexist in aqueous solutions, procedures to remove both are used at the same time. Deng *et al.*[114] used $Fe_2O_3$ or graphene nanosheets/magnetite to make MGO for the elimination of Cu(II) and dyes such as methylthioninium chloride and orange gelb, also magnetic rectorite and graphene nanosheets/magnetite.

(d) Abdi *et al.*[102] produced a magnetic graphene-based composite (MGC) in polyethersulfone polymers functioning as a membrane, which showed 99% dye rejection as well as eriochrome black T (EBT) adsorption from textile waste water.

### 3.3 Removal of radioactive metal ions

Much radioactive material is thrown into the aquatic environment as a result of nuclear and mining activities. This puts aquatic life in jeopardy.[111] Through water systems, the emitted fission product enters the food chain. Radionuclides are produced by anthropogenic tasks like ore processing, fertiliser use, and lignite burning in powder plants. As a result, an effective cure system for the elimination of long-lived radionuclides is required. Zhao used stacked GO-based nanosheets to achieve a supreme adsorption capacity ($q_{max}$) of 97.5 mg $g^{-1}$ for the adsorption of U(VI) ions. The performance of produced nanosheets, on the other hand, deteriorated because of agglomeration of GO nanosheets in the water.

Radioactive waste generated during production of nuclear energy and mining operations has a long-term impact on the environment. Sr-90, Cs-137, U-235, and I-129, which are generated as a by-product of the fission process, can set foot in the food chain *via* water system, and water contaminated by these radio nucleoids can infiltrate dirt and captivated by plants, eventually reaching animals and humans. Ore processing, lignite burning in power plants, and fertiliser use are all sources of radionuclides. Contamination of freshwater by these radio nucleoids is a major concern.

Zhao *et al.*[115] worked on it, and because GO-based nanosheets aggregate, functionalization of GO with magnetic materials was thought to be a successful way. For the adsorption of U, Sun *et al.*[97] created iron-rGO (nanosize zero valent) (VI). Lingamdinne *et al.*[116] created nickel ferrite-GO nanocomposites that can be used to treat U(VI) and Th(IV). MGO nanocomposites possess a good adsorption capability for both of these chemicals and may be reused up to five times.

### 3.4 Heavy metals removal

Heavy metals are one of the most common pollutants in water, and they can pose substantial health concerns to individuals who consume water contaminated with them. The adsorption method is employed because it is economical and efficient, although it has some limitations in terms of filtration and adsorbent regeneration. As a result, contrary spinel ferrites and their derivatives are employed as adsorbents instead of adsorbents because of their chemical and magnetic firmness, large surface porous structure, however nano-ferrites show less stability. As a result, hybrid materials made from ferrites and GO created superparamagnetic rMGO composites with a 99.9% adsorption capacity for As(III) and As(V). Arsenate adsorption from water having a ferric hydroxide-GO composite.[117] For adsorption of Cd(II), Cu(II) and Pb(II) from the aqueous environment, water soluble MGO produced through copper

Table 3 MGO-based nanomaterials in removal of heavy metals[a]

| Metal ions | Adsorbent | Maximum adsorption capacity (mg $g^{-1}$) | Conditions | Model (adsorption isotherm; kinetics) | Remarks |
|---|---|---|---|---|---|
| Cd | GO | 1792.60 | 303 K; pH 4.0 | Langmuir and Freundlich; pseudo second-order | • The equilibrium contact time is 120 minutes<br>• The GO is created by using amorphous graphite |
| | PAMAMs/GO | 253.81 | 298 K; pH 5.0 | Langmuir; pseudo second-order | • The adsorption mechanism gains equilibrium within 60 minutes<br>• The adsorbent dosage is 0.1 g |
| | Few-layered GO nanosheets | 106.30 | 303 K; pH 6.0 | Langmuir | • The dosage of adsorbent is 0.1 g $L^{-1}$<br>• The adsorption capability is strongly based on pH and humic acid |
| | GO/cellulose membranes | 26.8 | 298 K; pH 4.5 | Langmuir; pseudo second-order | • Better adsorption and no precipitation of metal hydroxides<br>• It can be utilized again up to ten cycles |
| Pb | Few-layered GO | 842.00 | 293 K; pH 6.0 | Langmuir | • pH value strongly affects the adsorption capacity<br>• The adsorption capacity is highly independent of ionic strength |
| | Graphene nanosheet | 476.19 | 298 K; pH 6.2 | Langmuir | • The equilibrium contact time is 35 minutes<br>• The dosage of adsorbent is 40 mg $L^{-1}$ |
| | Ag/GO | 312.57 | 298 K; pH 5.3 | Langmuir; pseudo second-order | • 0.05 mg of adsorbents used presented the maximum adsorption performance<br>• The equilibrium time for the lead adsorption is 50 minutes |
| Cu | Chitosan/SH/GO | 425.00 | 293 K; pH 5.0 | Freundlich; pseudo second-order | • The dosage of adsorbents is 0.2 mg $mL^{-1}$<br>• The adsorption efficiency is strongly dependent on pH, temperature and adsorbent dosage |
| | $TiO_2$/GO | 45.20 | 293 K; pH 6.0 | Langmuir | • The adsorption capacity is strongly based on the pH value |
| | GO aerogels | 19.65 | 298 K; pH 6.2 | Langmuir; pseudo second-order | • The dosage of adsorbents is 0.6 g $L^{-1}$<br>• It includes ion exchange mechanism |
| Cr | Chitosan/GO | 310.40 | 318 K; pH 3.0 | Redlich– Peterson/double exponential | • The adsorbent dosage is 0.5 g $L^{-1}$<br>• Both internal and external diffusion take place effectively in the adsorption technique |
| | $Fe_3O_4$/GO | 32.33 | 293 K; pH 4.5 | Langmuir; pseudo second-order | • pH value and ionic strength are the crucial factors to affect the adsorption capacities<br>• The adsorbent dosage is 0.2 g $L^{-1}$ |

[a] This table has been adapted/reproduced from ref. 119 with permission from Elsevier, copyright 2018.

catalyzed azide–alkyne cycloaddition is utilized. Composites of RGO and $MnO_2$ that can absorb mercury,[118] As(III) and As(V) elimination using $Fe_3O_4$–rGO–MnO composite. The composite improved adsorption and adsorption spots were achieved by reducing $MnO_2$ and $Fe_3O_4$ aggregation.

For water purification, metal oxides such as niobium pentaoxide ($Nb_2O_3$), titanium oxide ($TiO_2$), iron oxide ($Fe_2O_3$), and others are being used. For the absorption of pollutants from water, GO, rGO, and graphene combined with ZnO are examples. Chemical stability, non-toxicity, great electrical conductivity, greater surface area, outstanding mechanical strength, stiffness, ZnO nanocomposites[109] have large surface area and greater number of active sites. The saturation of graphene sheets over it by a simple solvothermal technique produces ZnO nanoparticles. The $Fe_2O_3$–rGO caused greater adsorption, and the reaction was exothermic and pH dependent.

The adsorption capacity of reduced magnetic graphene composites for all metal ions was found to be greater than that of non-reduced MGO. These can be used up to five times before needing to be replaced. When compared to GO and iron oxide alone, MGO boarded iron oxide demonstrated higher adsorption elimination of arsenic.[73]

List of many kinds of MGO nanocomposites that have been presented in literature for the remediation of contaminated aquatic environments, as well as their maximal sorption capabilities ($q_{max}$) are presented in Table 3.

# 4. Characterization

Before employing the GO membrane for filtering, it can be physically characterized to determine that it has the desired properties. The scanning electron microscope (SEM) was initially utilized to confirm the surface shape and layered structure of the GO membrane. Following are the techniques to characterize graphene-based membranes.

## 4.1 SEM analysis of GO and rGO

Surface fractures, defects, impurities, and corrosion were all evaluated using scanning electron microscopy (SEM). The extensive morphological examinations were carried out using a scanning electron microscope. SEM pictures of GO nanosheets are shown in Fig. 8. The wrinkles and folds of GO nanosheets are seen in the Fig. 8. This result proved that exfoliation of graphite oxide can form two-dimensional nanosheets of GO. Similar types of images have been reported in the literature.[120]

## 4.2 Raman spectroscopy for GO and rGO

When a molecule is bombarded with monochromatic light, Raman spectroscopy offers information based on the inelastic (Raman) scattering of the molecule. The Raman spectra of GO and rGO are presented in Fig. 9. In Fig. 9, two fundamental vibrations for GO and rGO could be seen in the region of 1100 and 1700 $cm^{-1}$. For GO and rGO, the D vibration band created by a breathing mode of j-point photons with $A_{1g}$ symmetry may be detected at 1348.31 and 1353.20 $cm^{-1}$, respectively. G vibration band from first-order scattering of $E_{2g}$ phonons by $sp^2$ carbon, on the other hand, was found at 1594.19 $cm^{-1}$ for GO and 1586.56 $cm^{-1}$ for rGO. The existence of stretching C–C bond, which is prevalent in all $sp^2$ carbon systems, also contributed to the G vibration band. The disorder bands and tangential bands are represented by the D and G bands in the Raman spectra Fig. 9. In addition, in Fig. 9, a broad and shifted to higher wavenumber of 2D band was detected for GO at 2716.77 $cm^{-1}$. As it is highly sensitive to graphene layer

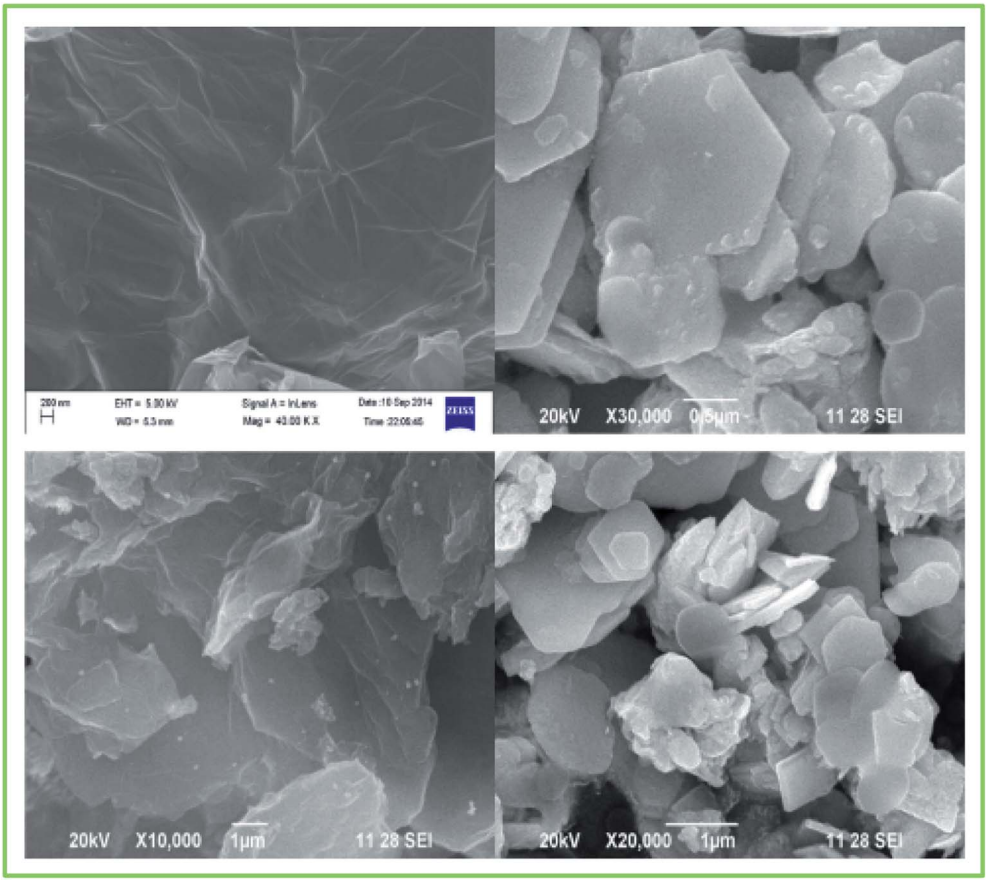


Fig. 8 SEM image of graphene oxide (GO) nanosheets. This figure has been adapted/reproduced from ref. 120 with permission from Elsevier, copyright 2020.

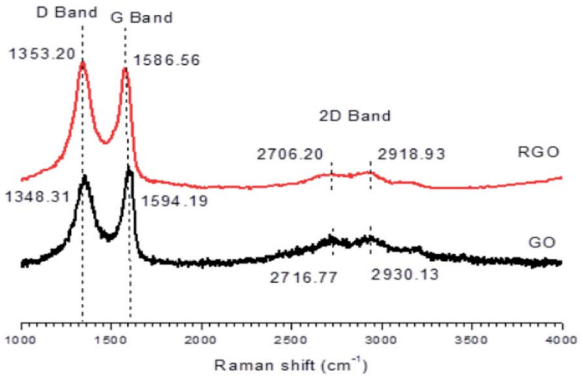


Fig. 9 Raman spectra of graphene oxide (GO), and reduced graphene oxide (rGO). This figure has been adapted/reproduced from ref. 121 with permission from American Institute of Physics, copyright 2017.

stacking, the 2D band can be utilised to find out layers of graphene (monolayer, double layer, and multilayers). Because monolayer graphene is generally found at 2679 $cm^{-1}$ from the spectra, the placement of the 2D band confirms that the generated GO was multilayer. Furthermore, the existence of O-containing moieties inhibits the graphene layer from stacking, resulting in the displaced location of the 2D band. RGO likewise possesses this 2D band at 2706.20 $cm^{-1}$, as illustrated in Fig. 9. This is due to after reduction from GO to rGO, there was less residual of O-containing moieties, causing the rGO to stack. Moreover, the location of the 2D band in this practical is little bit similar to the practical of Thakur and Karak, who revealed that phytochemicals derived from leaves, peels, or other parts of plants can reduce GO. As a reducing agent, phytochemicals were utilised instead of chemicals. The ID/IG ratio of GO was found to be 0.86. The ID/IG for rGO enhanced after reduction because of the restoration of $sp^2$ carbon, and mean sizes of $sp^2$ domains reduced. Higher D band intensity revealed that rGO had more isolated graphene domains than GO, possibly due to the elimination of oxygen moieties from GO during reduction.[121]

### 4.3 FT-IR analysis of MGO

FT-IR analysis was used to look at the surface functional groups. The vibrational peaks at 3392 and 1639 $cm^{-1}$ in the FT-IR of the MGO before adsorption are for the bending vibration of the –OH groups, as seen in Fig. 10. The Fe–O vibration is represented by the peak at 538. Some alterations in the MGO spectra appeared after As(III) adsorption. From 982 to 1180 $cm^{-1}$, a new band with lower intensity formed, which could be attributed to the creation of the Fe–As complex. Due to the replacement of –OH on the surface of MGO by As(III), the strength of the bending vibration of –OH was also reduced.[122]

### 4.4 UV-Visible spectroscopy of GO and rGO

The quantitative examination of how much a chemical compound absorbs light was done using UV-Vis Spectroscopy. Fig. 11 shows the UV-Vis spectra of GO and rGO. This found that their optical characteristics differed significantly. The absorption bands centered at 258 nm for GO and 297 nm for rGO are attributed to $\pi$–$\pi^*$ transitions of graphene's $\pi$ bonds. Because of the increase in the conjugation of rGO, the red-shifting of the GO peak from 258 to 297 nm of rGO indicates the occurrence of reduction.[123]

### 4.5 XRD analysis of graphite (Gt), GO and rGO

The spacing between two layers is a critical criterion for evaluating graphene structural information. In the XRD pattern of graphite oxide sheets, the diffraction peak seemed to be 11.88°, equivalent to a layer-to-layer distance of 0.8 nm, which is much larger than that of other graphite oxide sheets in Fig. 12a. The (0 0 1) peak centered at 11.88° corresponds to a distance of around 0.8 nm, which is the distance between the stacked GO sheets, and it is attributable to the high intercalating oxide functional groups of GO. This corresponds to the apparent thickness of a single layer of GO. This peak also supports your findings, which point to the production of GO. We also compared DTT's reduction efficiency to that of GO, a parent material, and

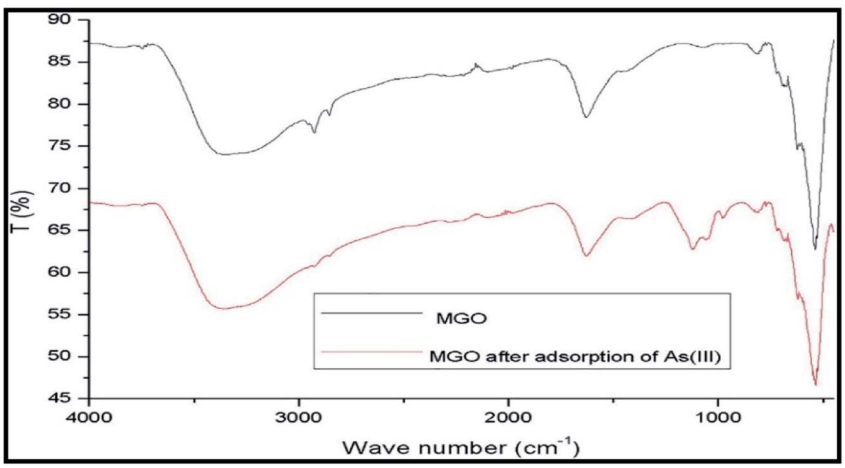


Fig. 10 Fourier transform infrared (FT-IR) spectrum for MGO before and after adsorption. This figure has been adapted/reproduced from ref. 122 with permission from Taylor & Francis, copyright 2019.

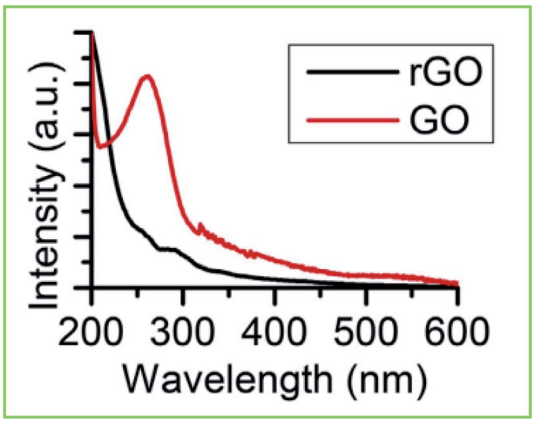


Fig. 11 UV-Vis absorption spectra of graphene oxide (GO), and reduced graphene oxide (rGO). This figure has been adapted/reproduced from ref. 123 with permission from Elsevier, copyright 2019.

hydrazine, a well-known chemical reducing agent. The XRD patterns of GO are compared to DTT-reduced samples Fig. 12b. The *d*-spacing of the GO is about 0.76 nm ($2\theta \approx 11.88$), due to the presence of oxygen-containing functional groups attached on both sides of the graphene sheet and atomic-scale roughness arising from structural defects ($sp^3$ bonding) generated on the originally atomically flat graphene sheet. After reduction of GO by DTT, the (*d* 0 0 2) peak of GO gradually disappears, whereas the broad diffraction peak observed from $2\theta \approx 25.7$, whereas hydrazine reduced graphene powder exhibits prominent diffraction peaks at $2\theta \approx 25.9$ corresponding to an interlayer spacing of 0.35 nm, which is notably different from pristine graphite, which is consistent with recent results on hydrazine chemical reduction of graphene oxide. The drop of the GO can be due to the shift in interlayer spacing, with the rGO pack being tighter than the GO. The interlayer gap reduces to 0.35 nm, indicating that exfoliation removes a significant amount of oxygen and water from the interlayer. This large surge in graphene is likewise indicative of a lack of long-range order. This research showed that graphene nanosheets were exfoliated into a monolayer or a few layers, resulting in a novel lattice structure that differed greatly from pristine graphite flakes and graphite oxide. Although complete reduction was observed, a small shoulder appeared in DTT reduced GO at $2\theta \approx 11.88$, indicating incomplete reduction of graphene oxide to graphene nanosheets or presumably induced by a bimodal or multimodal character of the interlayer spacing of RGO powder. This is due to the presence of residual oxygen and hydrogen, indicating incomplete reduction of graphene oxide to graphene nanosheets or presumably induced by a bimodal or multimodal character of the interlayer spacing of RGO powder.[124]

### 4.6 XPS analysis of GO

The existence of O-containing bonds in both GO and Fe–Mg hydroxide had been exploited to eliminate heavy metals mostly *via* complexation and ion exchange *via* $OH^-$ ions. Grafting highly oxygenated β-cyclodextrin functional groups onto GO has also successfully solved the problems of GO's high tendency to form polymerized layer structures. As a result, the high specific

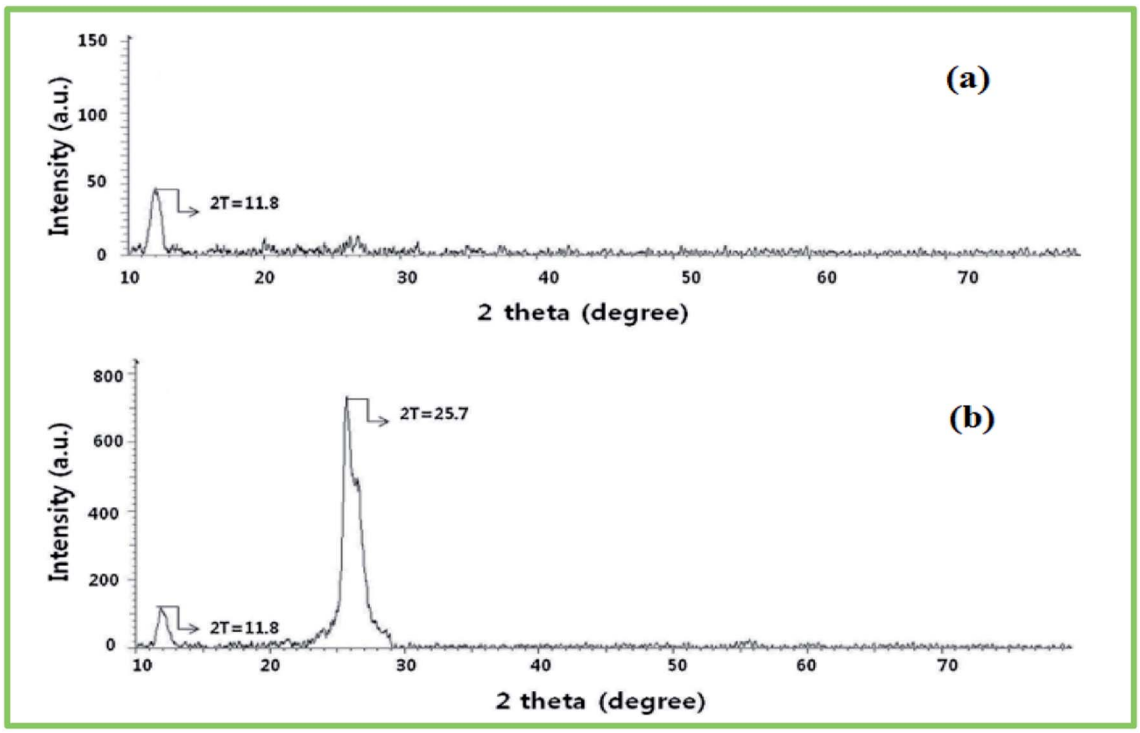


Fig. 12 X-ray diffraction patterns of (a) graphene oxide (GO), (b) reduced graphene oxide (rGO). This figure has been adapted/reproduced from ref. 124 with permission from Elsevier, copyright 2013.

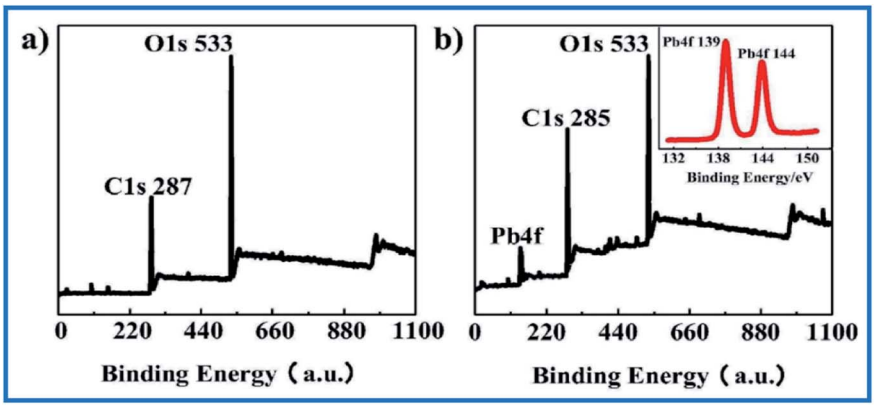


Fig. 13 XPS spectra of (a) before and (b) after adsorption of Pb(II) onto β-cyclodextrin enhanced GO. This figure has been adapted/reproduced from ref. 125 with permission from Elsevier, copyright 2020.

surface area was preserved and Pb(II) maximum adsorption capacity was raised to 149.56 mg $g^{-1}$ as shown in Fig. 13.[125]

## 5. Challenges

Graphene offers a wide range of commercial uses, although its use in industrial or commercial products has been limited thus far. For a variety of reasons, industries and other businesses have not embraced this miracle material. It is extremely difficult to generate graphene in big quantities without faults, however there are firms working on improving it.

Despite the fact that much research has been done and significant discoveries have been achieved in the discipline of graphene and graphene-based materials investigation, there are still a number of hurdles in commercializing graphene oxide membranes. These are;

(a) The membranes stability is a major issue. After the drawing process, the size of graphene oxide membranes decreases, causing instability. Work has been done to avoid this reduction problems, which can be resolved by depositing membranes in aqueous medium to avoid excessive drying[96,111] or using a top sacrificial coating during synthesis of membrane.[126,127]

(b) Recent study on improving the stability of graphene oxide membranes has shown that using ceramic material as a substrate improves membrane stability in aqueous medium by dismissing numerous multivalent ions that enable cross linking of graphene oxide sheets, but more work is needed to resolve this issue when the membrane is only at the sub micro level. Several researches have also found limitations in the characterization of graphene oxide membranes.

## 6. Conclusion and future perspective

The scarcity of fresh water, which is worsening day by day, emphasizes the need to find an effective material for wastewater treatment. In order to remediate contaminated water, graphene oxide, reduced graphene oxide and magnetic graphene oxide nanoparticles, and their composites are recently studied. MGO-based materials have long been utilized in the treatment of water, like iron oxide for the elimination of radioactive metals from water are gaining popularity. Desalination and the removal of organic pollutants applications have seen significant use of graphene and graphene oxide to improve membrane characteristics. Antimicrobial, antifouling, mechanical strength, selectivity, water flux, and thermal characteristics of GO upgraded after fusion into membrane. Photo-catalysts such as zinc and titanium oxide, in combination with graphene, can be utilised to eliminate organic contaminants. Heavy metals can be removed, and monovalent and divalent ions can be separated using graphene oxide membranes. Various methods of manufacturing have been developed. The GO nanosheets are the most fundamental building blocks for the production of GO aided membranes, however, its limitations, such as stability concerns, should be addressed. Strengthening the commercial production of ultrathin GO membranes is one of the most difficult tasks we face today; we must find a compromise between costs and synthesizing operations simplicity. GO membranes could be one the most crucial technologies for addressing the impending global water crises.

The following are the primary judgements and subsequent views of the current state of MGO-based nanocomposites for sustainable water purification.

(a) The key advantages of MGOs as adsorbents are their outstanding magnetic property, cost-effectiveness, tunable property, magnetic property, and viability.

(b) Surface charge and textural qualities, thermal and surface moieties have all influenced the adsorption properties of MGO.

(c) Regeneration of rGO and MGOs can be accomplished through changing the pH of the solution or adding low mass acid/base or alcohols.

(d) In comparison to other adsorbents previously appeared in literature, MGO's composites have equivalent or even though stronger adsorption and reformation capability.

(e) Many GO, rGO, and MGOs showed good properties throughout a wide pH range, indicating that they could be used in practical applications.

(f) Furthermore, the better adsorption effectiveness of the adsorbents during the processing of wastewater including heavy metals and radionuclides and organic dyes and farming contaminants could contribute to a more sustainable community.

## Conflicts of interest

There are no conflicts of interest stated by the authors.

## Acknowledgements

Dr Faiza Asghar is highly grateful to University of Wah for providing necessary facilities.

## References

1 B. S. Lalia, V. Kochkodan, R. Hashaikeh and N. Hilal, *Desalination*, 2013, **326**, 77–95.
2 P. H. Gleick, *Int. Secur.*, 1993, **18**, 79–112.
3 S. Kar, R. C. Bindal and P. K. Tewari, *Nano. Today.*, 2012, **7**, 385–389.
4 X. Qu, J. Brame, Q. P. Li and P. J. J. Alvarez, *Acc. Chem. Res.*, 2013, **46**, 834–843.
5 D. Nutbeam and I. Kickbusch, *Health. Promot. Int.*, 1998, **4**, 349–364.
6 M. Shannon, P. W. Bohn, M. Elimelech, J. G. Georgiadis, B. J. Marinas and A. M. Mayes, *Nature*, 2008, **452**, 301–310.
7 T. D. Phan, J. C. R. Smart, S. J. Capon, W. L. Hadwen and O. Sahin, *Environ. Model. Softw.*, 2016, **85**, 98–111.
8 M. Nurasyikin, W. J. Lau and A. F. Ismail, *Desalination*, 2012, **287**, 228–237.
9 R. P. Schwarzenbach, T. Egli, T. B. Hofstetter, U. V. Gunten and B. Wehrli, *Annu. Rev. Environ. Resour.*, 2010, **35**, 109–136.
10 R. Yang, J. Xu, G. Ozaydin-Ince, S. Y. Wong and K. K. Gleason, *Chem. Mater.*, 2011, **23**, 1263–1272.
11 E. Alayemieka and S. Lee, *Desalin. Water. Treat.*, 2012, **45**, 84–90.
12 C. Gabelich, J. Frankin, F. Gerringer, K. Ishida and I. Suffet, *J. Memb. Sci.*, 2005, **258**, 64–70.
13 Y. Yao, P. Zhang, C. Jiang, R. M. DuChanois, X. Zhang and M. Elimelech, *Nat. Sustain.*, 2021, **4**, 138–146.
14 J. E. Cadotte, R. J. Petersen, R. E. Larson and E. E. Erickson, *Desalination*, 1980, **32**, 25–31.
15 S. H. Maruf, D. U. Ahn, J. Pellegrino, J. P. Killgore, A. R. Greenberg and Y. Ding, *J. Memb. Sci.*, 2012, **405–406**, 167–175.
16 K. P. Lee, T. C. Arnot and D. Mattia, *J. Membr. Sci.*, 2011, **370**, 1–22.
17 J. Gascon, F. Kapteijn, B. Zornoza, V. Sebastián, C. Casado and J. Coronas, *Chem. Mater.*, 2012, **24**, 2829–2844.
18 Y. Wei, Y. Zhang, X. Gao, Z. Ma, X. Wang and C. Gao, *Carbon*, 2018, **139**, 964–981.
19 T. Humplik, J. Lee, S. C. O'Hern, B. A. Fellman, M. A. Baig, S. F. Hassan, M. A. Atieh, F. Rahman, T. Laoui, R. Karnik and E. N. Wang, *J. Nanotechnol.*, 2011, **22**, 292001–292019.
20 P. S. Goh, A. F. Ismail and B. C. Ng, *Desalination*, 2013, **308**, 2–14.
21 Y. Liu, B. Xie, Z. Zhang, Q. Zheng and Z. Xu, *J. Mech. Phys. Solids.*, 2012, **60**(4), 591–605.
22 W. Hu, C. Peng, W. Luo, M. Lv, X. Li, D. Li, Q. Huang and C. Fan, *ACS Nano*, 2010, **4**(7), 4317–4323.
23 A. Jankovic, S. Erakovic, M. V. Sekulic, V. M. Stankovic, S. J. Park and K. Y. Rhee, *Prog. Org. Coat.*, 2015, **83**, 1–10.
24 S. J. Kim, S. H. Ko, K. H. Kang and J. Han, *Nat. Nanotechnol.*, 2010, **5**, 297–301.
25 A. T. Habte and D. W. Ayele, *Adv. Mater. Sci. Eng.*, 2019, **2019**, 1–9.
26 A. K. Mishra and S. Ramaprabhu, *Desalination*, 2011, **282**, 39–45.
27 Z. Yang, Y. Zhou, Z. Feng, X. Rui, T. Zhang and Z. Zhang, *Polymers*, 2019, **11**(8), 1252–1274.
28 A. Mushtaq, H. B. Mukhtar and A. M. Shariff, *Procedia Eng.*, 2016, **148**, 11–17.
29 P. Hou, C. Liu and H. Cheng, *Carbon*, 2008, **46**(15), 2003–2025.
30 A. Eatemadi, H. Daraee, H. Karimkhanloo, M. Kouhi, N. Zarghami, A. Akbarzadeh, M. Abasi, Y. Hanifehpour and S. W. Joo, *Nanoscale Res. Lett.*, 2014, 393–406.
31 B. Xu, S. Yue, Z. Sui, X. Zhang, S. Hou, G. Cao and Y. Yang, *Energy Environ. Sci.*, 2011, **4**, 2826–2830.
32 S. Pei and H. Cheng, *Carbon*, 2012, **50**, 3210–3228.
33 Q. A. Khan, A. Shaur, T. A. Khan, Y. F. Joya and M. S. Awan, *Cogent Chem.*, 2017, **3**, 1298980–1298989.
34 R. S. Rajaura, I. Singhal, K. N. Sharma and S. Srivastava, *Rev. Sci. Instrum.*, 2019, **90**, 123903–123915.
35 M. S. Saravanan, S. P. Babu, K. Sivaprasad and M. Jagannatham, *Int. J. Eng. Sci. Technol.*, 2010, **2**(5), 100–108.
36 R. Shah, A. Kausar, B. Muhammad and S. Shah, *Polym. Plast. Technol. Eng.*, 2015, **54**, 173–183.
37 Z. U. Khan, A. Kausar, H. Ullah, A. Badshah and W. U. Khan, *J. Plast. Film Sheeting*, 2016, **32**, 336–379.
38 A. Kausar, I. Rafique and B. Muhammad, *Polym. Plast. Technol. Eng.*, 2016, **55**, 1167–1191.
39 R. Sattar, A. Kausar and M. Saddiq, *J. Plast. Film Sheeting*, 2015, **31**, 186–224.
40 S. Imtiaz, M. Saddiq, A. Kausar, S. T. Muntha, J. Ambreen and I. Bibi, *Chin. J. Polym. Sci.*, 2018, **36**, 445–461.
41 J. Zhou, X. Song, B. Shui and S. Wang, *Coatings*, 2021, **11**, 1040–1059.
42 M. Zunita, *Membranes*, 2021, **11**, 269–284.
43 A. Matin, Z. Khan, S. M. J. Zaidi and M. C. Boyce, *Desalination*, 2011, **281**, 1–16.
44 M. T. Yagub, T. K. Sen, S. Afroze and H. M. Ang, *Adv. Colloid Interface Sci.*, 2014, **209**, 172–184.
45 F. Arshad, M. Selvaraj, J. Zain, F. Banat and M. A. Hajja, *Sep. Purif. Technol.*, 2018, **209**, 870–880.
46 T. S. Sreeprasad, S. M. Maliyekkal, K. P. Lisha and T. Pradeep, *J. Hazard. Mater.*, 2011, **186**, 921–931.
47 L. F. Greenlee, D. F. Lawler, B. D. Freeman, B. Marrot and P. Moulin, *Water Res.*, 2009, **43**, 2317–2348.

48 M. C. Amiri and M. Samiei, *Desalination*, 2007, **207**, 361–369.
49 A. Schinwald, F. A. Murphy, A. Jones, W. MacNee and K. Donaldson, *ACS Nano*, 2012, **1**(6), 736–746.
50 Y. Huang, J. Liang and Y. Chen, *J. Mater. Chem.*, 2012, **22**, 3671–3679.
51 S. Bae, H. Kim, Y. Lee, X. Xu, J. Park, Y. Zheng, J. Balakrishnan, T. Lei, H. R. Kim, Y. I. Song, Y. Kim, K. S. Kim, B. Ozyilmaz, J. Ahn, B. H. Hong and S. Iijima, *Nat. Nanotechnol.*, 2010, **8**, 574–578.
52 F. Perreault, M. E. Tousley and M. Elimelech, *Environ. Sci. Technol. Lett.*, 2014, **1**, 71–76.
53 K. Cao, Z. Jiang, J. Zhao, C. Zhao, C. Gao, F. Pan, B. Wang, X. Cao and J. Yang, *J. Membr. Sci.*, 2014, **469**, 272–283.
54 N. Wei, X. Peng and Z. Xu, *ACS Appl. Mater. Interfaces*, 2014, **8**, 5877–5883.
55 J. Prasek, J. Drbohlavova, J. Chomoucka, J. Hubalek, O. Jasek, V. Adam and R. Kizek, *J. Mater. Chem.*, 2011, **21**, 15872–15884.
56 A. Oberlin, M. Endo and T. Koyama, *J. Cryst. Growth*, 1976, **32**, 335–349.
57 S. Iijima, *Nature*, 1991, **354**, 56–58.
58 S. Stankovich, D. A. Dikin, R. D. Piner, K. A. Kohlhaas, A. Kleinhammes, Y. Jia, Y. Wu, S. T. Nguyen and R. S. Ruoff, *Carbon*, 2007, **45**, 1558–1565.
59 S. P. Surwade, S. N. Smirnov, I. V. Vlassiouk, R. R. Unocic, G. M. Veith, S. Dai and S. M. Mahurin, *Nat. Nanotechnol.*, 2015, **10**, 459–464.
60 M. Khalil, B. M. Jan, C. W. Tong and M. A. Berawi, *Appl. Energy.*, 2017, **191**, 287–310.
61 H. M. Hegab and L. Zou, *J. Membr. Sci.*, 2015, **484**, 95–106.
62 S. P. Koenig, L. Wang, J. Pellegrino and J. S. Bunch, *Nat. Nanotechnol.*, 2012, **7**, 728–732.
63 M. Hu and B. Mi, *Environ. Sci. Technol.*, 2013, **47**, 3715–3723.
64 Y. Nam, J. Kang, J. Jang, J. Bae, H. Jung and D. Kim, *Membranes*, 2021, **11**, 793–810.
65 J. S. Bunch, S. S. Verbridge, J. S. Alden, A. M. Zande, J. M. Parpia, H. G. Craighead and P. L. McEuen, *Nano Lett.*, 2008, **8**, 2458–2462.
66 D. A. Dikin, S. Stankovich, E. J. Zimney, R. D. Piner, G. H. B. Dommett, G. Evmenenko, S. T. Nguyen and R. S. Ruoff, *Nature*, 2007, **448**, 457–460.
67 Y. Zhu, S. Murali, W. Cai, X. Li, J. W. Suk, J. R. Potts and R. S. Ruoff, *Adv. Mater.*, 2010, **22**, 3906–3924.
68 C. Chen, Q. Yang, Y. Yang, W. Lv, Y. Wen, P. Hou, M. Wang and H. Cheng, *Adv. Mater.*, 2009, **21**, 3007–3011.
69 D. W. Boukhvalov, M. I. Katsnelson and Y. Son, *Nano Lett.*, 2013, **8**, 3930–3935.
70 N. F. D. Aba, J. Y. Chong, B. Wang, C. Mattevi and K. Li, *J. Membr. Sci.*, 2015, **484**, 87–94.
71 K. Goh, L. Setiawan, L. Wei, R. Si, A. G. Fane, R. Wang and Y. Chen, *J. Membr. Sci.*, 2015, **474**, 244–253.
72 S. Liu, F. Yao, O. Oderinde, Z. Zhang and G. Fu, *Carbohydr. Polym.*, 2017, **174**, 392–399.
73 A. W. Hauser and P. Schwerdtfeger, *J. Phys. Chem. Lett.*, 2012, **3**, 209–213.
74 O. Akhavan and E. Ghaderi, *ACS Nano*, 2010, **4**, 5731–5736.
75 S. Kang, M. Pinault, L. D. Pfefferle and M. Elimelech, *Langmuir*, 2007, **23**, 8670–8673.
76 V. B. Mohan, K. Lau, D. Hui and D. Bhattacharyya, *Compos. B. Eng.*, 2018, **142**, 200–220.
77 P. Sun, M. Zhu, K. Wang, M. Zhong, J. Wei, D. Wu, Z. Xu and H. Zhu, *ACS Nano*, 2013, **7**, 428–437.
78 A. Enotiadis, K. Angjeli, N. Baldino, I. Nicotera and D. Gournis, *Small*, 2012, **8**, 3338–3349.
79 Y. Heo, H. Im and J. Kim, *J. Memb. Sci.*, 2013, **425–426**, 11–22.
80 T. Szabo, A. Szeri and I. Dekany, *Carbon*, 2005, **43**, 87–94.
81 H. He, J. Klinowski, M. Forster and A. Lerf, *Chem. Phys. Lett.*, 1998, **287**, 53–56.
82 A. Lerf, H. He, M. Forster and J. Klinowski, *J. Phys. Chem. B*, 1998, **102**, 4477–4482.
83 S. Park and R. S. Ruoff, *Nat. Nanotechnol.*, 2009, **4**, 217–224.
84 C. Xu, A. Cui, Y. Xu and X. Fu, *Carbon*, 2013, **62**, 465–471.
85 N. Wang, S. Ji, G. Zhang, J. Li and L. Wang, *Chem. Eng. J.*, 2012, **213**, 318–329.
86 R. R. Nairh, H. A. Wu, P. N. Jayaram, I. V. Grigorieva and A. K. Geim, *Science*, 2012, **335**, 442–444.
87 Z. Wang, H. Yu, J. Xia, F. Zhang, F. Li, Y. Xia and L. Yanhui, *Desalination*, 2012, **299**, 50–54.
88 J. Zhang, Z. Xu, W. Mai, C. Min, B. Zhou, M. Shan, Y. Li, C. Yang, Z. Wang and X. Qian, *J. Mater. Chem. A.*, 2013, **9**, 3101–3111.
89 X. Luo, C. Wang, S. Luo, R. Dong, X. Tu and G. Zeng, *Chem. Eng. J.*, 2012, **187**, 45–52.
90 J. Liang, Y. Huang, L. Zhang, Y. Wang, Y. Ma, T. Guo and Y. Chen, *Adv. Funct. Mater.*, 2009, **19**, 2297–2302.
91 P. Bernardo, E. Drioli and G. Golemme, *Ind. Eng. Chem. Res.*, 2009, **48**, 4638–4663.
92 R. W. Baker, *Ind. Eng. Chem. Res.*, 2002, **41**, 1393–1411.
93 L. Xiao-Lei, T. Shuo, L. Ke-Da, W. Ya-Song, W. Ping and T. Zhi-Jian, *Acta Phys.-Chim. Sin.*, 2016, **32**, 1495–1500.
94 H. Li, Z. Song, X. Zhang, Y. Huang, S. Li, Y. Mao, H. J. Ploehn, Y. Bao and M. Yu, *Science*, 2013, **342**, 95–98.
95 H. W. Kim, H. W. Yoon, S. Yoon, B. M. Yoo, B. K. Ahn, Y. H. Cho, H. J. Shin, H. Yang, U. Paik, S. Kwon, J. Choi and H. B. Park, *Science*, 2013, **342**, 91–95.
96 S. C. O'Hern, M. S. H. Boutilier, J. Idrobo, Y. Song, J. Kong, T. Laoui, M. Atieh and R. Karnik, *Nano Lett.*, 2014, **14**, 1234–1241.
97 P. Sun, F. Zheng, M. Zhu, Z. Song, K. Wang, M. Zhong, D. Wu, R. B. Little, Z. Xu and H. Zhu, *ACS Nano*, 2014, **8**, 850–859.
98 M. Khayet, *Desalination*, 2013, **308**, 89–101.
99 W. Yu, L. Sisi, Y. Haiyan and L. Jie, *RSC Adv.*, 2020, **10**, 15328–15345.
100 S. Pei and H. Cheng, *Carbon*, 2012, **50**(9), 3210–3228.
101 X. Gao, J. Jang and S. Nagase, *J. Phys. Chem. C*, 2010, **114**, 832–842.
102 G. Abdi, A. Alizadeh, S. Zinadini and G. Moradi, *J. Membr. Sci.*, 2018, **552**, 326–335.
103 H. Li, S. Liu, J. Zhao and N. Feng, *Colloid. Surface. Physicochem. Eng. Aspect.*, 2016, **494**, 222–227.

104 W. Zhang, X. Shi, Y. Zhang, W. Gu, B. Li and Y. Xian, *J. Mater. Chem. A.*, 2013, **5**, 1745–1753.
105 V. K. Gupta, S. Agarwal, M. Asif, A. Fakhri and N. Sadeghi, *J. Colloid Interface Sci.*, 2017, **497**, 193–200.
106 K. P. Singh, S. Gupta, A. K. Singh and S. Sinha, *J. Hazard. Mater.*, 2011, **186**, 1462–1473.
107 W. Intrchom, S. Roy, M. S. Humoud and S. Mitra, *Membranes*, 2018, **8**, 63–75.
108 K. L. Klarich, N. C. Pflug, E. M. DeWald, M. L. Hladik, D. W. Kolpin, D. M. Cwiertny and G. H. Lefevre, *Environ. Sci. Technol. Lett.*, 2017, **4**, 168–173.
109 K. Buesseler, M. Aoyama and M. Fukasawa, *Environ. Sci. Technol.*, 2011, **45**, 9931–9935.
110 L. Zhou, X. Yang, B. Yang, X. Zuo, G. Li, A. Feng, H. Tang, H. Zhang, M. Wu, Y. Ma, S. Jin, Z. Sun and X. Chen, *J. Power Sources*, 2014, **272**, 639–646.
111 V. Chandra, J. Park, Y. Chun, J. W. Lee, I. Hwang and K. S. Kim, *ACS Nano*, 2010, **4**, 3979–3986.
112 G. Liu, X. Yang, T. Li, Y. She, S. Wang, J. Wang, M. Zhang, F. Jin, M. Jin, H. Shao and M. Shi, *Mater. Lett.*, 2015, **160**, 472–475.
113 P. K. Boruah, B. Sharma, N. Hussain and M. R. Das, *Chemosphere*, 2017, **168**, 1058–1067.
114 X. Deng, L. Lü, H. Li and F. Luo, *J. Hazard. Mater.*, 2010, **183**, 923–930.
115 Y. Zhao, Z. Xu, M. Shan, C. Min, B. Zhou, Y. Li, B. Li, L. Liu and X. Qian, *Sep. Purif. Technol.*, 2013, **103**, 78–83.
116 L. P. Lingamdinne, J. R. Koduru, Y. Chang and R. R. Karri, *J. Mol. Liq.*, 2018, **250**, 202–211.
117 M. Aminuzzaman, L. P. Ying, W. Goh and A. Watanabe, *Bull. Mater. Sci.*, 2018, **41**, 50–60.
118 J. Y. Chong, N. F. D. Aba, B. Wang, C. Mattevi and K. Li, *Sci. Rep.*, 2015, **5**, 1–11.
119 J. Y. Lim, N. M. Mubarak, E. C. Abdullah, S. Nizamuddin, M. Khalid and M. Inamuddin, *J. Ind. Eng. Chem.*, 2018, **66**(25), 29–44.
120 M. Muniyalakshmi, K. Sethuraman and D. Silambarasan, *Mater. Today. Proceedings.*, 2020, **21**, 408–410.
121 N. M. S. Hidayah, W. Liu, C. Lai, N. Z. Noriman, C. Khe, U. Hashim and H. C. Lee, *AIP Conf. Proc.*, 2017, **1892**, 150002–150011.
122 A. I. A. Sherlala, A. A. A. Raman and M. M. Bello, *Environ. Technol.*, 2019, **40**, 1508–1516.
123 G. G. Gebreegziabher, A. S. Asemahegne, D. W. Ayele, M. Dhakshnamoorthy and A. Kumar, *Mater. Today Chem.*, 2019, **12**, 233–239.
124 S. Gurunathan, J. W. Han, A. A. Dayem, V. Eppakayala, M. Park, D. Kwon and J. Kim, *J. Ind. Eng. Chem.*, 2013, **19**, 1280–1288.
125 S. Z. N. Ahmad, W. N. W. Salleh, A. F. Ismail, N. Yusof, M. Z. M. Yusop and F. Aziz, *Chemosphere*, 2020, **248**, 126008–126024.
126 Y. Yuan and S. Gurunathan, *Int. J. Nanomedicine.*, 2017, **12**, 6537–6558.
127 S. Zhang, W. Xu, M. Zeng, J. Li, J. Li, J. Xu and X. Wang, *J. Mater. Chem. A.*, 2013, **38**, 11691–11697.